AD-A115 490 COLORADO STATE UNIV FORT COLLINS DEPT OF CHEMISTRY F/G 20/8
MOLECULAR AGGREGATES IN CRYOGENIC SOLUTIONS,(U)
JUL 81 M W SCHAUER, J LEE, E R BERNSTEIN N00014-79-C-0647
UNCLASSIFIED TR-5 NL

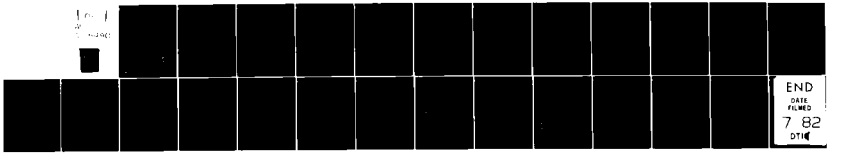

(12)

OFFICE OF NAVAL RESEARCH
Contract N00014-79-C-0647

Technical Report No. 5

MOLECULAR AGGREGATES IN CRYOGENIC SOLUTIONS

by

M.W. Schauer, J. Lee, and E.R. Bernstein

Prepared for Publication in
The Journal of Chemical Physics

Department of Chemistry
Colorado State University
Fort Collins, Colorado 80523

7 July 1981

in the molecular jet system, such as $(H_2O)_x$, $(C_6H_6)_x$, etc., these latter results are not unrelated to those presented here. Supersonic molecular jet spectra of various types of clusters have evidenced both red ($(C_6H_6)_2$ and $He_x\ C_2N_4H_2$) and blue ($He_x\ I_2$) shifts from the unperturbed isolated solute molecular spectra. Such shifts are central to the identification of aggregates as will be shown below.

In this work some general observations serve to distinguish solutions of aggregates from solutions of monomers. Rapid deposition into a precooled sample cell is required to generate an aggregate solution. Such a solution yields an absorption spectrum which is always red shifted from the absorption spectrum of a solution of monomers. Spectra of monomer solutions may be either red or blue shifted from that of the low pressure ($\sim$1 torr) gas, however. The red shift of the aggregate system always parallels (but is not always identical to) that observed for a pure crystal at comparable temperatures. If typical aggregate solutions are warmed to more than 120K, spectra corresponding to aggregates begin to decrease slowly in intensity and, concomitantly, features associated with monomer spectra begin to appear. Cooling a solution of monomers shows that this process is, of course, not reversible; solute simply precipitates, as usual, without the reappearance of spectra associated with aggregate solutions. The aggregation process is trapped in a rapidly cooled and deposited non-equilibrium low temperature liquid. After several hours at low temperature (1-12 hours depending on the particular system), aggregate spectra begin to decrease in intensity and precipitate can be seen in the solution. The appearance of red shifted, temperature and time dependent spectra allows identification of an aggregate solution.

In this report, experimental procedures and results concerning the study of aggregates are presented. Absorption spectra of solutions of the following solutes and solvents have been studied: pyrazine/C_3H_8; benzene/NF_3, C_3H_8, N_2, CO, CF_4; and osmium tetroxide/NF_3, CH_4, C_3H_8. In order to obtain some qualitative estimation of aggregate size light scattering experiments were also performed on solutions of pyrazine/C_3H_8, benzene/CF_4 benzene/NF_3, and benzene/C_3H_8. The nature of these non-equilibrium molecular clusters in solution will be addressed.

II. EXPERIMENTAL

Purification and sample handling procedures for these experiments are similar to those reported previously[8]. Purification of solutes was accomplished by trap to trap vacuum distillation through molecular sieve. Solvents are in general similarly treated[8], being distilled through a 130K molecular sieve trap directly into an outgassed 7ℓ stainless steel holding can. For light scattering experiments the solvent distillation is done twice. Solvent and solute are mixed in the vapor phase in the holding can which then is allowed to equilibrate for at least 24 hours before deposition to ensure thorough mixing of the two constituents. Deviation from this mixing procedure, however, did not yield different results for aggregate spectra.

Absorption apparatus is the same as that described previously. Solutions, held at set temperatures between 65 and 220K by a closed cycle mechanical refrigerator, and irradiated with a 500W Xenon lamp filtered with various appropriate Hoya glass filters placed in water. A cooled RCA C31000M photomultiplier tube with photon counting electronics is used to detect the absorption.

Light scattering experiments use a argon ion laser with an intracavity etalon for single mode 5145Å output. Powers at the sample are

typically about 50mw. Brillouin and Rayleigh (correlation) scattering are observed simultaneously in order to determine the best portion of the scattered light to detect for Rayleigh studies. This apparatus is described elsewhere[9]. The best correlation spectra are observed in the case for which Brillouin peaks are maximized in intensity with respect to the central Rayleigh peak observed through the interferometer. Correlation light scattering is detected through two pin holes (100μm) separated by about 0.5m with the first pinhole about 0.25m from the collection lens. Scattered light is analyzed by a Malvern real time auto correlator and an HP 9845S computer for curve fitting and graphic output.

III. RESULTS

Absorption spectra of pyrazine in propane at ca. 100K evidence the characteristics associated with aggregate solutions described earlier. These data show the $^1B_{3u}$ origin of pyrazine shifted 505cm^{-1} to the red of the monomer (150K) origin and 819cm^{-1} to the red of the gas phase origin[10] (see fig. 1). Aside from this overall shift the three spectra, gas, monomer solution and aggregate solution spectra are superimposible. Assignments of vibronic features are indicated in fig. 1 and table I.

Warming the low temperature solution causes the aggregate spectrum to decrease in intensity. As the aggregate spectrum disappears, the monomer spectrum begins to appear and increases in intensity until reaching its equilibrium value. Upon subsequent cooling of the solution back to 100K, aggregate spectra do not reappear; monomer spectra and some precipitate are observed. No spectra can be observed associated with any amount of precipitate floating in solution.

Spectra were also obtained as a function of concentration. At 100K only monomer spectra are seen for 3.5, 5, 7ppm and below 2ppm no spectra were observed at all. At 8ppm clear pyrazine/propane solutions show aggregate

spectra and concentrations of 10, 12, 14ppm yield aggregate spectra of increased intensity. A graph of this concentration-intensity dependence at fixed temperature is given in fig. 2.

Light scattering experiments were carried out on pyrazine/propane and benzene/NF_3, CF_4, C_3H_8 solutions in order to estimate mean aggregate size[9]. A relaxation curve of the decay of the time correlation function for the system can be fit to a single exponential decay function (fig. 3); from this process a relaxation time may be calculated. Using the relations,

$$1/\tau = Dq^2$$

$$D = \frac{kT}{6\pi\eta_v a}$$

$$q^2 = 4\left(\frac{2\pi n_r}{\lambda}\right)^2 \left(\sin\frac{\theta}{2}\right)^2$$

in which:

τ = relaxation time, D = diffusion constant, q = scattering vector, k = Boltzmann's constant, T = temperature, η_v = viscosity, a = particle diameter, n_r = refractive index for 5145Å, λ = wave length of light, and θ = scatter angle (θ=90°), a particle size can be calculated assuming a spherical particle shape. The observed relaxation for the pyrazine/C_3H_8 aggregate solution, at 100K ± 10K and independent of concentration from 3.5 to 15ppm, is found to be 20 ± 2 msec. This corresponds to a particle size of roughly 10^3Å. Similar results are obtained for benzene/NF_3 and CF_4 but no aggregates are found in C_6H_6/C_3H_8 solution at any temperature.

Solution and aggregate spectra for C_6H_6/NF_3 are presented in fig. 4 which shows the temperature dependence of the spectra of an 8ppm sample. The aggregate spectrum was obtained in a 90K solution and the monomer spectrum was obtained in a 140K solution. Table II summarizes the assignments for both aggregates and monomers.

Fig. 5 depicts three spectra of the first two one photon allowed bands of OsO_4: gas phase at 300K; monomer solution at 150K in C_3H_8; and aggregate solution in NF_3 at 90K. Fig. 6 shows monomer and aggregate spectra of OsO_4 in C_3H_8 at 150K and 120K, respectively. In comparison to the gas phase spectrum two distinct regions may be classified in these condensed phase spectra. In monomeric solutions the first six bands show a red shift with respect to the gas phase spectrum while the last 12 bands evidence a blue shift from the corresponding gas phase values. For aggregate solutions (C_3H_8 and NF_3) all bands are red shifted, by varying amounts however, from the gas phase spectrum but in such a manner as to preserve this decomposition. These data are summarized in table III. OsO_4 is itself not soluble enough in NF_3 to produce an observable monomer solution spectrum at 140K.

IV. DISCUSSION

The most extensive study of solute aggregate formation is for pyrazine; both absorption and light scattering measurements have been made for this system at many temperatures and concentrations. In the discussion given below most phenomena will be presented for pyrazine; observations dealing with C_6H_6 and OsO_4 solutions will be presented only as they pertain to these individual systems.

A. Pyrazine

The red shift of the pyrazine aggregate spectrum is close to that of the pyrazine crystal spectrum[11]. This indicates that aggregation provides an environment similar to that found in the crystal.

The deposition procedure has been observed to be important for the production of aggregates. If mixtures are cooled slowly under equilibrium conditions, precipitation ensues without observable amounts (in absorption or light scattering experiments) of aggregate production. With rapid, non-equilibrium deposition, supersaturated solutions are produced which trap

aggregates in solution and prevent precipitation. As the temperature is raised above 120K for $C_4N_2H_4/C_3H_8$ aggregates are broken up by increased solubility of monomers and the overall increase in kT. Of course, both energy and entropy considerations control the solvation process.

Line widths for the aggregate spectra are roughly as one might expect; similar to a poor crystal at ~ 100K. The lack of emission from aggregate species is also understandable in this light. The implication, as shown below, is that most aggregates are fairly large with $n \geq 10^3$. The fact that (hydrocarbon) solution and aggregate line widths are similar may be indicative of similar short range repulsive interactions in both systems. The long range forces, due mostly to C-C and C-N potentials, are, or course, different in aggregate and solution as is evident from the different gas to liquid and gas to aggregate red shifts for pyrazine.

Light scattering experiments demonstrate that there is a sharp decrease in the size of scatters with an increase in temperature. At roughly 140K nearly all the aggregates have dissolved and the number density of effective scatters has decreased to the point at which trace amounts of dust become the primary scatters. Single pyrazine molecules are too small to be observed in this experiment.

The two different techniques for observing the presence of aggregates in solution, absorption and light scattering, have distinct sensitivities for each of the solution species. For example, at low concentrations (<5ppm) absorption spectra show no aggregate peaks but light scattering indicates the presence of 10^3Å size particles. At about 5-7ppm monomer absorption is obscured by aggregate features (fig. 1). Near 15ppm $C_4N_2H_4/C_3H_8$ microcrystals can be observed floating in solution at 100K. Upon warming these solutions to 150K and subsequently cooling them neither technique can observe aggregates, even under conditions for which precipitate can be visually observed floating in solution. Monomers are still observed in absorption but light scattering data are unattainable.

Within experimental error, the size of aggregate particles in solution does not depend significantly on concentration; high concentrations of pyrazine simply produced stronger light scattering but always with roughly the same relaxation time. Higher concentration solutions are observed, however, to yield precipitation at higher temperatures.

Size determination of aggregates is most likely an order of magnitude

estimate. There are two major sources of error. The primary source of error is probably the assumption of spherical shape which leads to a diameter of 10^3Å. A sphere of this diameter would include of the order of 10^6 pyrazine molecules. If the particles are disk or cylinder shaped, the number of molecules per particle could be several orders of magnitude less. Moreover, a different shape would yield a different relationship between measured relaxation time and effective particle size. The most probable shape of these aggregates is, of course, not known; however, hints taken from rapid crystallization processes could favor cylindrical rods with large length to diameter ratios. A further complication for the determination of particle size is that there may exist in solution a broad continuum of distribution of sizes. If this were the case, one might expect that size distribution for a given solution would depend fairly strongly on initial concentration. This was certainly not observed in any of the light scattering experiments in the concentration range 3-15ppm. It may well be, however, that average relaxation times are not sensitive enough to changes in the most probable size distribution to evidence this polydispersivity. Thus, the measured times may be dominated by the largest particles in the distribution.

B. Benzene

The previous report from our laboratory on cryogenic liquid solutions dealt with the first excited singlet state of benzene[8]; aggregates were not identified for C_6H_6 in CO, N_2, CF_4, CH_4, C_2H_6, and C_3H_8. Nonetheless, C_6H_6/NF_3 solutions clearly show that at low temperature aggregation of C_6H_6 does indeed occur with a size close to that determined for pyrazine. The monomer spectrum (fig. 2 bottom) of C_6H_6/NF_3 shows two solvent effects which distinguish this system from other C_6H_6 solutions: a small ($\sim$80cm^{-1}) gas to liquid shift and a small band width (FWHH $\sim$ 100cm^{-1}). Other solvents

produce roughly 200cm^{-1} line widths and -275cm^{-1} gas to liquid shifts. In addition, this spectrum behaves much like that described for the pyrazine monomer: it is stable, reversible, and independent of deposition procedure. Again line widths and gas to aggregate shifts strongly suggest a close similarity between the aggregate and crystalline state and an aggregate size of $n \geq 10^3$.

Appearance of aggregate spectra for C_6H_6/NF_3 (fig. 2 and table II) raises questions concerning spectra of C_6H_6 in other solutions[8]. In the case of the solvents C_2H_6 and C_3H_8 all spectra observed can be attributed to monomers for the following three reasons: 1) both solvents have high boiling points and thus are good solvents (the calculated solubility at 150K is roughly 4×10^{-2}); 2) spectra are completely temperature independent; and 3) spectra of C_6H_6/C_2H_6 or C_3H_8 are time independent at any temperature between 85K and 200K. Due to the high solubility of C_6H_6 in these two solvents it is quite unlikely that the aggregation phenomenon can be observed. In fact, light scattering experiments reveal no detectable particle size at low temperature, thus eliminating the possibility that the monomer and aggregate spectra overlap.

CO, N_2, CF_4, and CH_4, on the other hand, have low boiling points and are relatively poor solvents for benzene. Moreover, the short liquid range makes it quite difficult to study temperature dependent spectra and gas to liquid and gas to crystal (aggregate) shifts are quite similar for these systems (ca. -250cm^{-1}). Unfortunately, light scattering studies for these systems are difficult to perform because the low solubility usually yields some particulate matter even at low concentrations.

C. OsO_4

Aggregation of OsO_4 is also found in C_3H_8 and NF_3 solvents at 90K. Both sets of features (A through F and G through R in fig. 5, 6 and table III) now evidence a red shift. Such results show that the OsO_4 aggregates, and indeed other aggregates in general, are crystal-like and not as affected by the solvent environment as monomers are.

The observation of both red (lower energy bands A through F) and blue (higher energy bands G through R) shifts for solution spectra with respect to gas phase spectra of OsO_4 (see table III and fig. 5) raises the question of the appropriate assignment of these transitions. These shift data clearly divide the bands into two electronic transitions. The two one photon allowed lowest observed OsO_4 transitions have been frequently discussed with respect to their orbital origin. It seems generally agreed that the first transition takes an electron from the highest filled $1t_1$ orbital to the lowest unfilled 2e orbital; T_1 and T_2 states are thereby created[12]. The second transition may involve either $1t_1$ to unfilled $4t_2$ or $3t_2$ (second highest filled orbital) to 2e. The 2e and $4t_2$ orbitals are essentially non-bonding metal d-orbitals split by the O_4^{-8} tetrahedral crystal field. Presently, the $(3t_2 \rightarrow 2e)$ T_2 assignment appears to be favored[13]. While it is clear that these two transitions involve different orbital sets, it is not apparent from the gas to liquid shift data which set is to be preferred for the higher energy one.

V. CONCLUSION

The major point made in this presentation is that for low temperature deposition and poor solvents a supersaturated non-equilibrium situation obtains in which aggregates of solute are formed as a precursor to complete precipitation. Aggregates are recognized by light scattering-particle size determination and by characteristic large crystal-like red shifts from both gas phase and solution spectra. Further studies are underway to elucidate the nature of the nucleation and growth process and to determine the actual shape(s) of such systems.

REFERENCES

1. B.H. Robinson, A.S. Löffler and G. Schwarz, J. Chem. Soc. Farad. Trans. I 71, 815 (1975).
2. S.I. Chan, M.P. Schweizer, P.O.P. Ts'o, and G.K. Helmkamp, J. Amer. Chem. Soc. 86, 4182 (1964).
3. a) E.R. Buckle, Farad. Discuss. Chem. Soc. 61, 7 (1976); b) M.R. Hoare and J. McInnes, Farad. Discuss. Chem. Soc. 61, 12 (1976).
4. E. Donaghue and J.H. Gibbs, J. Chem. Phys. 74, 2975 (1981).
5. A.M. Lockett III, J. Chem. Phys. 72, 4822 (1980).
6. Y. Singh and F.F. Abraham, J. Chem. Phys. 67, 537 (1977).
7. a) D.H. Levy, L. Wharton and R.E. Smalley, Chemical and Biochemical Applications of Lasers, Vol. II, pp. 1-41 (1977); b) A.W. Castleman, Jr., P.M. Holland and R.G. Keesee, J. Chem. Phys. 68, 1760 (1978); c) R.R. Gamache and P.E. Cade, J. Chem. Phys. 74, 5197 (1981); d) M.P. Casassa, D.S. Bomse and K.C. Janda, J. Chem. Phys. 74, 5044 (1981).
8. E.R. Bernstein and J. Lee, J. Chem. Phys. 74, 3159 (1981).
9. B.J. Berne and R. Pecora, Dynamic Light Scattering, (John Wiley and Sons, Inc., 1976).
10. Y. Udagawa, M. Ito and I. Suzuka, Chem. Phys. 46, 237 (1980).
11. E.F. Zalewski, D.S. McClure and D.L. Narva, J. Chem. Phys. 61, 2964 (1974).
12. a) K. Swift and E.R. Bernstein, J. Chem. Phys. 74, 5981 (1981); b) E.J. Wells, A.D. Jordan, D.S. Alderdice and I.G. Ross, Aust. J. Chem. 20, 2315 (1967).
13. a) E. Diemann and A. Müller, Chem. Phys. Lett. 19, 538 (1973); b) J.L. Roebber, R.N. Wiener and A. Russell, J. Chem. Phys. 60, 3166 (1974); c) P. Quested, D.J. Robbins, P. Day and R.G. Denning, Chem. Phys. Lett. 22, 158 (1973).

TABLE I

Assignments, energies, and gas to liquid red-shift for solutions of pyrazine in propane. Errors in absolute energies are estimated to be $\pm 15 cm^{-1}$.

Assignment	ENERGY (cm^{-1})	Red-shift from gas phase (cm^{-1})
Aggregate (100K)		
$^1B_{3u}$ origin	30057	819
$6a_0^1$	30646	813
$6a_0^2$	31227	815
$8a_0^1$	31406	843
$6a_0^3$	31786	839
$8a_0^1 6a_0^1$	31989	843
Solution (150K)		
origin	30562	314
$6a_0^1$	31142	316
$6a_0^2$	31723	319
$8a_0^1$	31933	316
$6a_0^3$	32299	326
$8a_0^1 6a_0^1$	32503	329
Gas (300K)		
origin	30876	
$6a_0^1$	31459	
$6a_0^2$	32042	
$8a_0^1$	32249	
$6a_0^3$	32625	
$8a_0^1 6a_0^1$	32832	

TABLE II

Absorption data for C_6H_6 in NF_3 at 90K (aggregate) and 140K (monomer-solution). Gas phase data are also given comparison. All values are in cm^{-1}.

Gas phase	Solution(140K)		Aggregate(90K)		Assignment
300K	Frequency	gas to liquid shift	Frequency	gas to liquid shift	
38612	38531	-81	38318	-294	6^1_0
39534	39451	-83	39250	-284	$6^1_0 1^1_0$
40456	40381	-75	40181	-275	$6^1_0 1^2_0$

TABLE III

Average gas to liquid shift for OsO_4 in cm^{-1}.

Solvents / Bands[a]	C_3H_8 Monomer	C_3H_8 Aggregate	NF_3 Aggregate
A-F	-144	-286	-211
G-R	228		

a - labels in figs. 5 and 6 and ref. 12b.

FIGURE CAPTIONS

FIGURE 1

Absorption spectra of pyrazine in propane:

a) aggregate spectrum at 100K;

b) monomer spectrum at 150K;

c) vapor spectrum at 300K.

FIGURE 2

Plot of intensity of the absorption spectra measured as the height of the origin peak vs. concentration of pyrazine in propane deposited at 100K. The first 3 points correspond to monomer spectra and the last 3 points correspond to aggregate spectra.

FIGURE 3

Plot of the normalized correlation function for a solution of pyrazine aggregates in propane at 3.5ppm and 100K. The solid line is a least squares fit to a single exponential function yielding a correlation time of τ=20msec.

FIGURE 4

Spectra of benzene in NF_3: A) aggregate solution (8ppm) spectra taken at 90K; B) monomer solution (8ppm) taken at 140K.

FIGURE 5

Absorption spectra of OsO_4:

A. OsO_4/C_3H_8 monomer spectrum at 8ppm and 150K;

B. OsO_4/NF_3 aggregate spectrum at 8ppm and 90K;

C. OsO_4 gas phase spectrum at 4°C (notation of ref. 12b is employed here and in text).

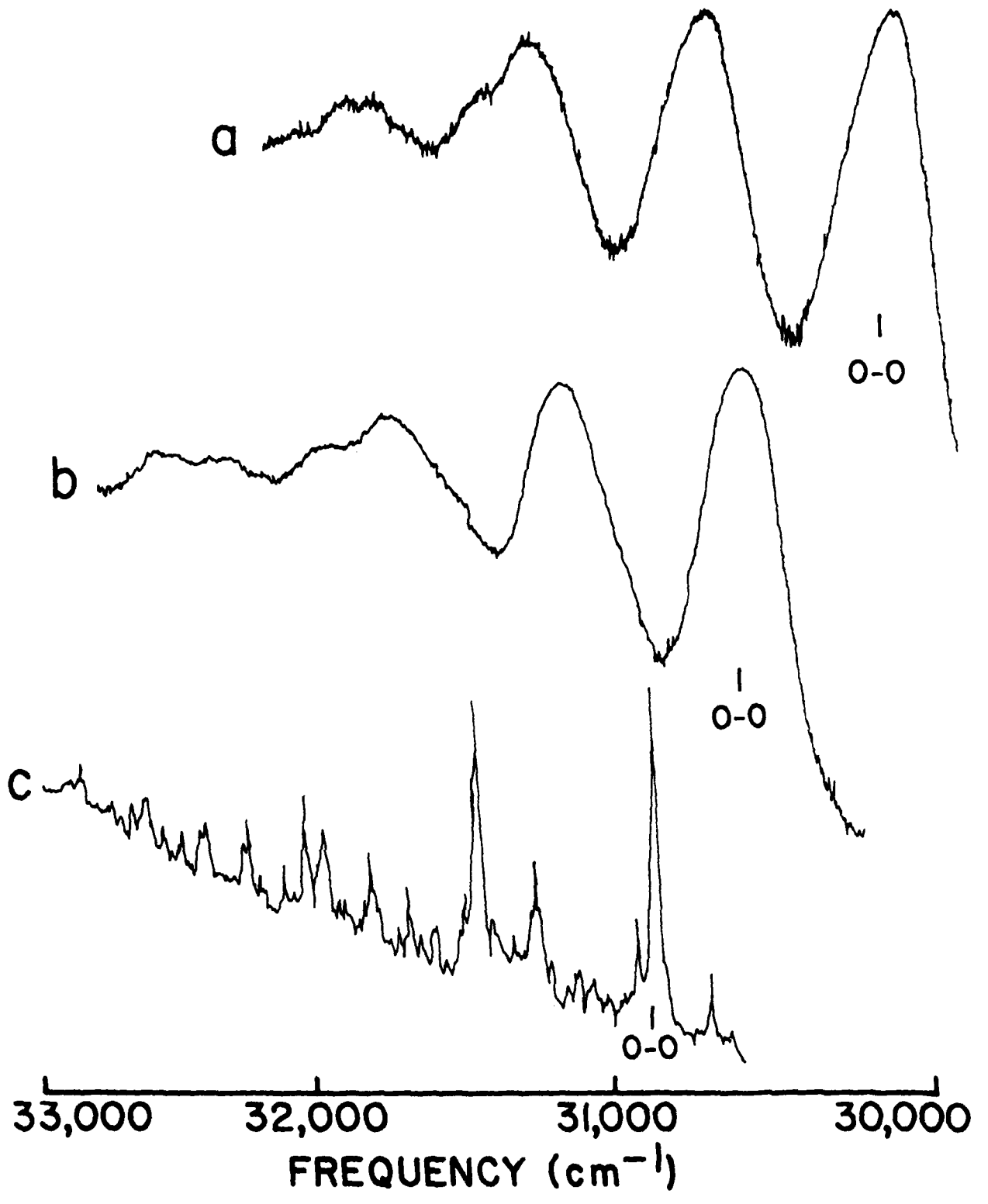
a
0-0
b
0-0
c
0-0
33,000
32,000
31,000
30,000
FREQUENCY (cm⁻¹)

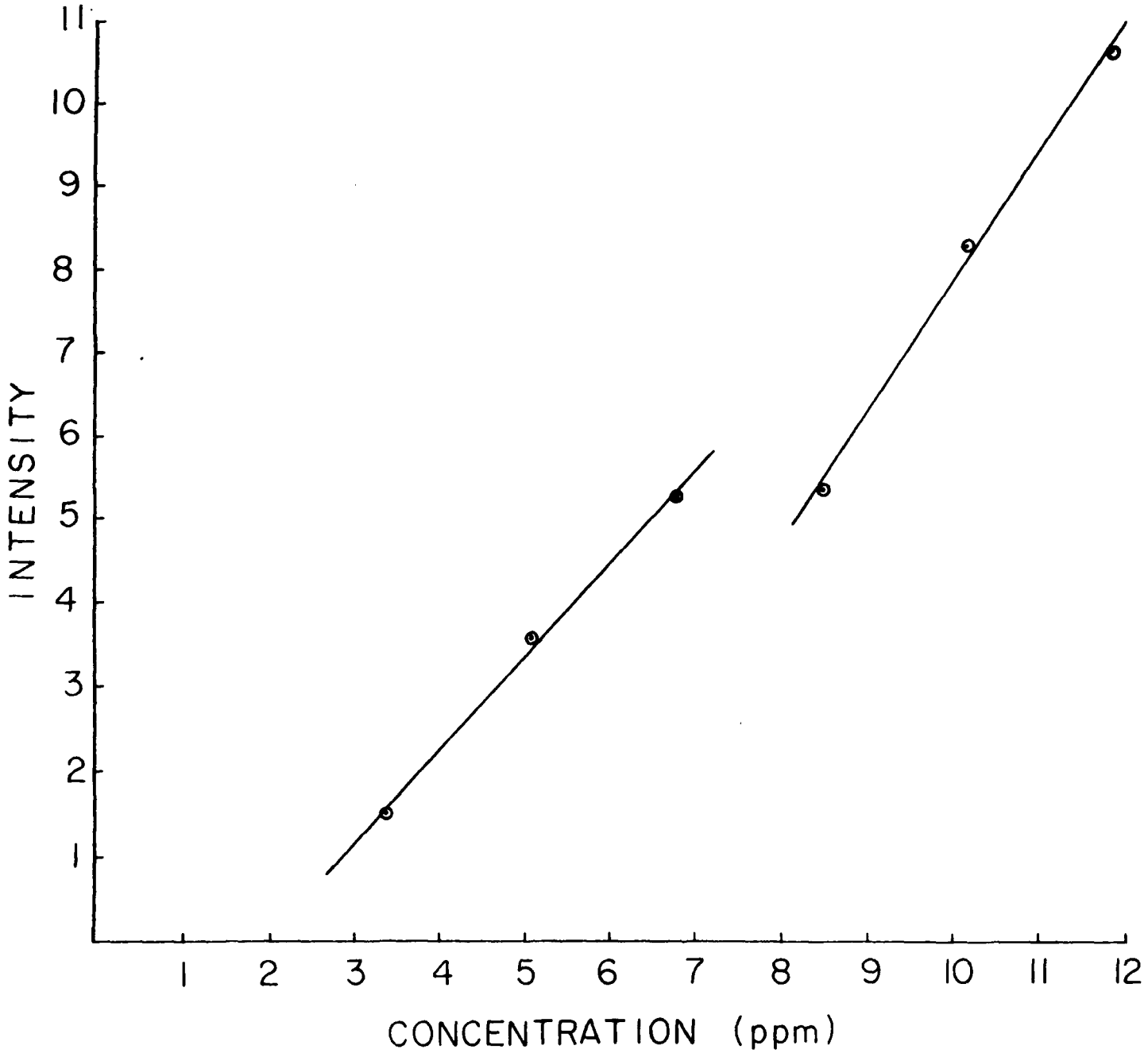
INTENSITY
1
2
3
4
5
6
7
8
9
10
11
1
2
3
4
5
6
7
8
9
10
11
12
CONCENTRATION (ppm)

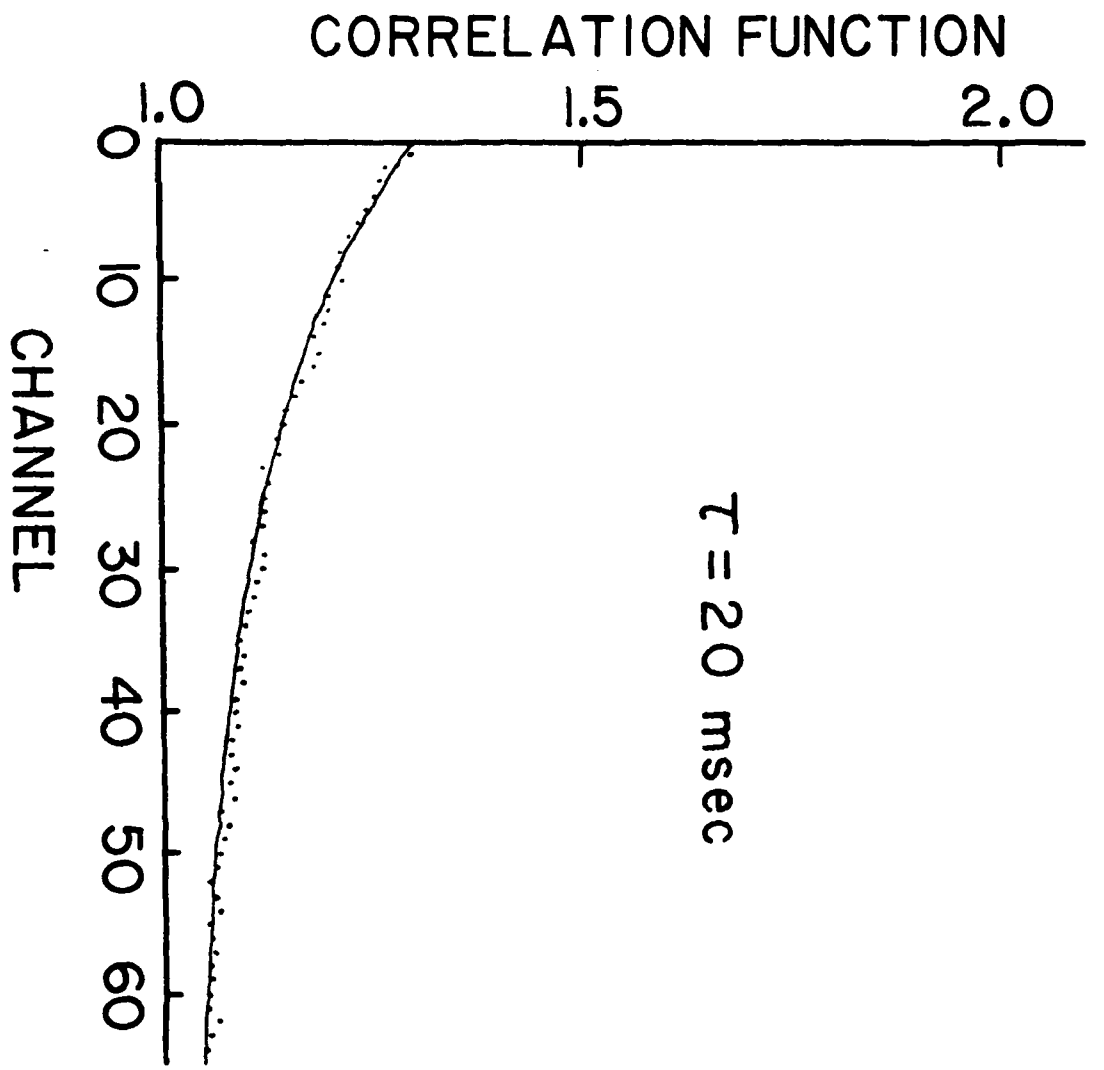
CORRELATION FUNCTION
1.0
1.5
2.0
0
10
20
30
40
50
60
CHANNEL
τ = 20 msec

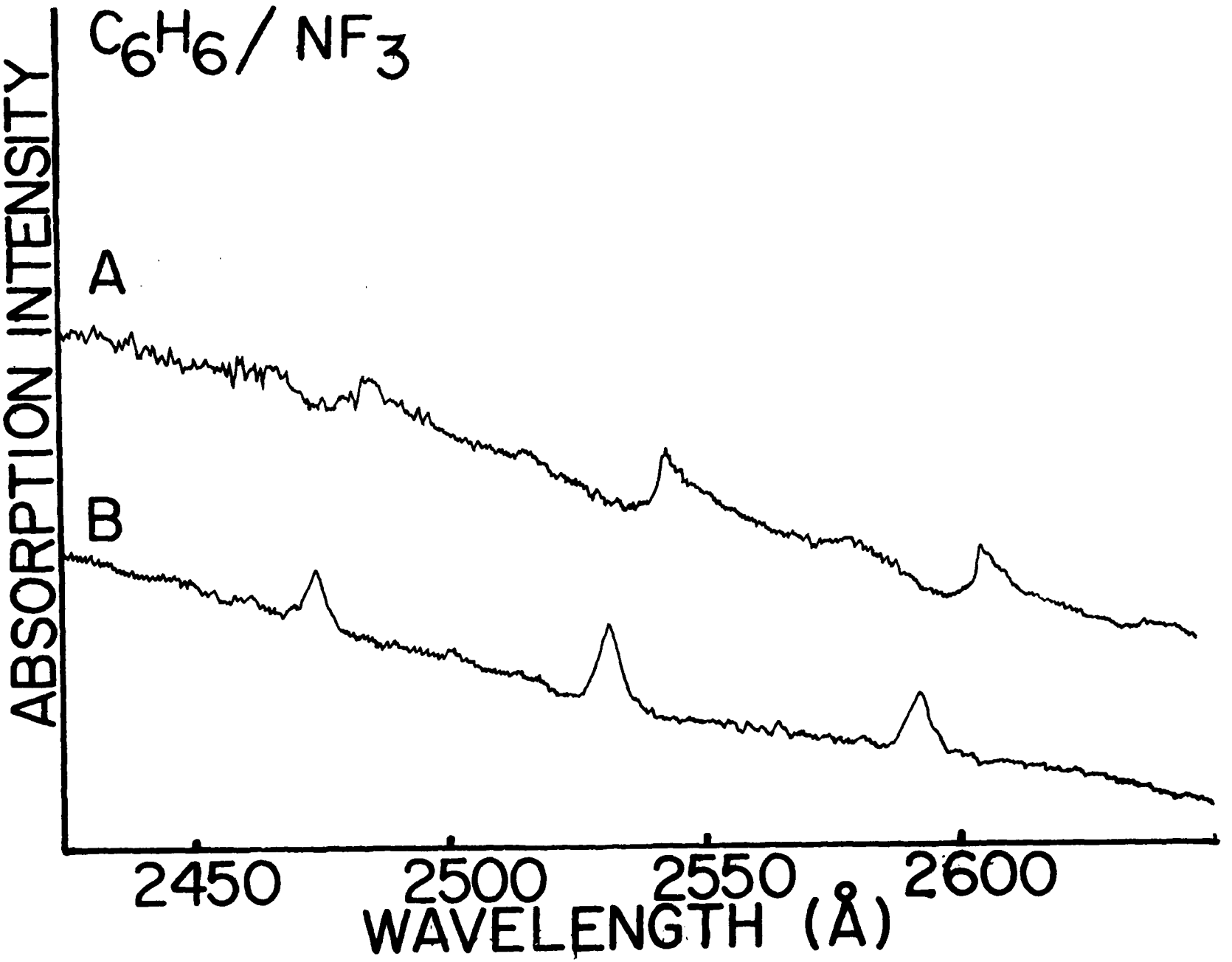
C_6H_6 / NF_3
ABSORPTION INTENSITY
A
B
2450
2500
2550
2600
WAVELENGTH (Å)

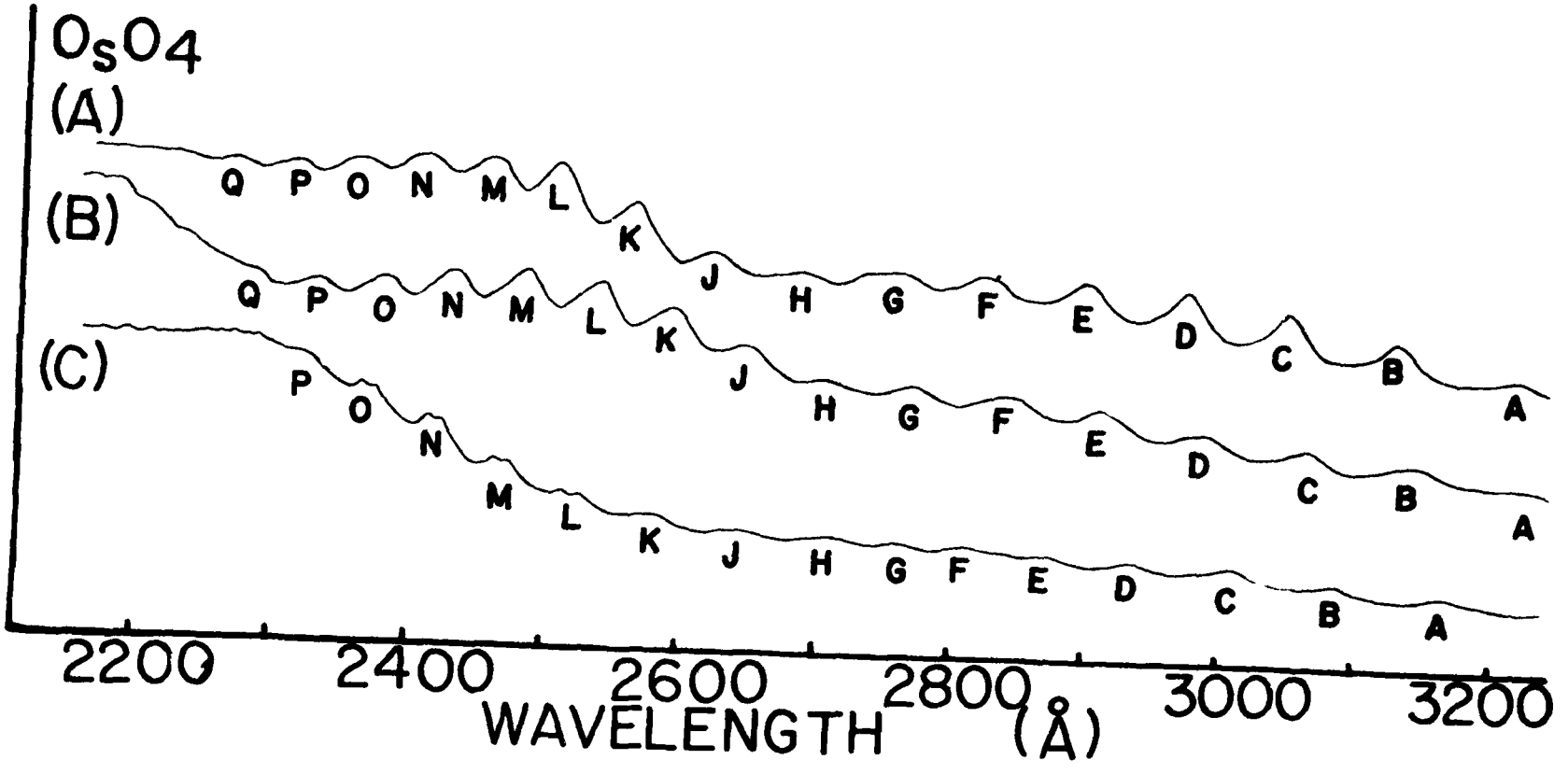
OsO4
(A)
(B)
(C)
Q P O N M L K J H G F E D C B A
Q P O N M L K J H G F E D C B A
P O N M L K J H G F E D C B A
2200
2400
2600
2800
3000
3200
WAVELENGTH (Å)

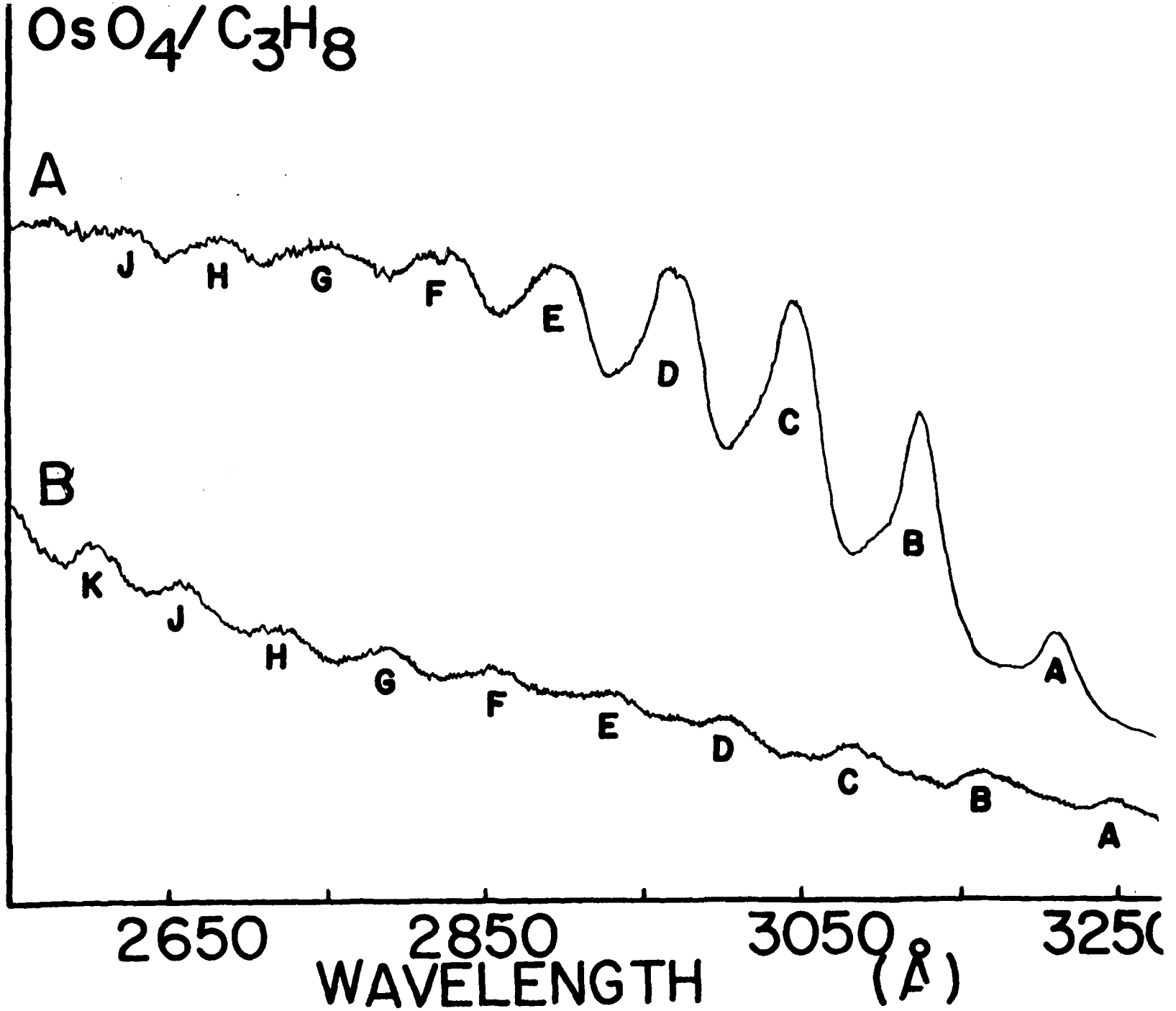
OsO_4/C_3H_8
A
J
H
G
F
E
D
C
B
A
B
K
J
H
G
F
E
D
C
B
A
2650
2850
3050
3250
WAVELENGTH (Å)

SP482-3/A23

472:GAN:716:ddc
78u472-608

TECHNICAL REPORT DISTRIBUTION LIST, 051A

	No. Copies
Dr. M. A. El-Sayed Department of Chemistry University of California, Los Angeles Los Angeles, California 90024	1
Dr. C. A. Heller Naval Weapons Center Code 6059 China Lake, California 93555	1
Dr. J. R. MacDonald Chemistry Division Naval Research Laboratory Code 6110 Washington, D.C. 20375	1
Dr. G. B. Schuster Chemistry Department University of Illinois Urbana, Illinois 61801	1
Dr. A. Adamson Department of Chemistry University of Southern California Los Angeles, California 90007	1
Dr. M. S. Wrighton Department of Chemistry Massachusetts Institute of Technology Cambridge, Massachusetts 02139	1
Dr. M. Rauhut Chemical Research Division American Cyanamid Company Bound Brook, New Jersey 08805	1
Dr. J. I. Zink Department of Chemistry University of California, Los Angeles Los Angeles, California 90024	1
Dr. D. Haarer IBM San Jose Research Center 5600 Cottle Road San Jose, California 95143	1
Dr. John Cooper Code 6130 Naval Research Laboratory Washington, D.C. 20375	1
Dr. William M. Jackson Department of Chemistry Howard University Washington, DC 20059	1
Dr. George E. Walraffen Department of Chemistry Howard University Washington, DC 20059	1

TECHNICAL REPORT DISTRIBUTION LIST, GEN

	No. Copies
Mr. James Kelley DTNSRDC Code 2803 Annapolis, Maryland 21402	1
Mr. A. M. Anzalone Administrative Librarian PLASTEC/ARRADCOM Bldg 3401 Dover, New Jersey 07801	1

SP472-3/A1

472:GAN:716:enj
78u472-608

TECHNICAL REPORT DISTRIBUTION LIST, GEN

	No. Copies
Office of Naval Research Attn: Code 472 800 North Quincy Street Arlington, Virginia 22217	2
ONR Western Regional Office Attn: Dr. R. J. Marcus 1030 East Green Street Pasadena, California 91106	1
ONR Eastern Regional Office Attn: Dr. L. H. Peebles Building 114, Section D 666 Summer Street Boston, Massachusetts 02210	1
Director, Naval Research Laboratory Attn: Code 6100 Washington, D.C. 20390	1
The Assistant Secretary of the Navy (RE&S) Department of the Navy Room 4E736, Pentagon Washington, D.C. 20350	1
Commander, Naval Air Systems Command Attn: Code 310C (H. Rosenwasser) Department of the Navy Washington, D.C. 20360	1
Defense Technical Information Center Building 5, Cameron Station Alexandria, Virginia 22314	12
Dr. Fred Saalfeld Chemistry Division, Code 6100 Naval Research Laboratory Washington, D.C. 20375	1
U.S. Army Research Office Attn: CRD-AA-IP P.O. Box 1211 Research Triangle Park, N.C. 27709	1
Naval Ocean Systems Center Attn: Mr. Joe McCartney San Diego, California 92152	1
Naval Weapons Center Attn: Dr. A. B. Amster, Chemistry Division China Lake, California 93555	1
Naval Civil Engineering Laboratory Attn: Dr. R. W. Drisko Port Hueneme, California 93401	1
Department of Physics & Chemistry Naval Postgraduate School Monterey, California 93940	1
Scientific Advisor Commandant of the Marine Corps (Code RD-1) Washington, D.C. 20380	1
Naval Ship Research and Development Center Attn: Dr. G. Bosmajian, Applied Chemistry Division Annapolis, Maryland 21401	1
Naval Ocean Systems Center Attn: Dr. S. Yamamoto, Marine Sciences Division San Diego, California 91232	1
Mr. John Boyle Materials Branch Naval Ship Engineering Center Philadelphia, Pennsylvania 19112	1

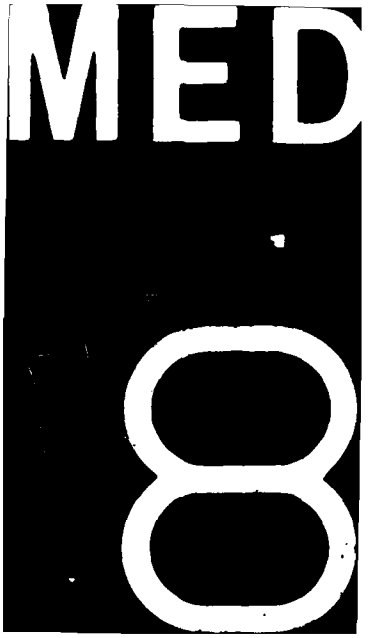
MED
8